

Doppler shift estimation methods in mobile communication systems

Hua Jingyu You Xiaohu

(National Mobile Communications Research Laboratory, Southeast University, Nanjing 210096, China)

Abstract: Several Doppler shift estimators, including mean logarithm envelope difference (MLED) method, auto-correlation function (ACF) method, zero crossing rate (ZCR) method and mean square phase difference (MSPD) method are discussed and compared. The estimation principle and theoretical estimation bias of these estimators under Rayleigh fading channels are analyzed; furthermore, the Cramer Rao bound (CRB) of Doppler shift estimation is deduced, and a novel modification method based on two-dimensional polynomial fitting is proposed to reduce the Doppler shift estimation bias. We verify our algorithms with the Monte Carlo computer simulation; simulation results show better variance performance of modified methods than those of the original methods. In addition, the applicable situations of these estimators are discussed.

Key words: Doppler shift; beyond the third generation (B3G); Cramer Rao bound

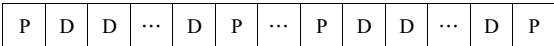
Rapid fading is a central problem in mobile communications^[1]. It degrades the bit error rate (BER), and frequently introduces an irreducible BER, or error floor. Using pilot signals to mitigate the effects of fading has been studied by many researchers. By the appropriate pilot signals we can track the fading.

The fading rate of the channel depends on the maximum Doppler shift f_d , and the Doppler shift is related to the velocity of the mobile terminal (MT). According to the requirement of 3G/B3G system, mobile terminals should operate in the velocity range from 0 to 500 km/h. Hence the knowledge or efficient estimation of the velocity of the MT is of great importance in mobile communication and ultimately will provide good handoff performance^[2], good power control performance^[3] and effective dynamic channel estimation^[4]. In order to estimate the velocity of an MT, Holtzman used the square envelope characteristic^[2]; Xiao used the channel correlation characteristic^[5]. In addition, there are estimators based on level crossing rate (LCR) and diversity reception^[6,7], etc. The limitation of these schemes is that the estimation accuracy is greatly affected by the velocity or signal-to-noise ratio (SNR) or power control or carrier frequency offset; all these should be considered in practice.

In this paper, several Doppler shift estimators are discussed, and the estimation bias is analyzed theoretically. Furthermore, a novel modification based on polynomial fit is proposed to improve estimation accuracy and Cramer Rao bound (CRB) is derived for comparison. The algorithms are verified with the Monte Carlo simulation, and the accurate and robust estimation results are observed in a wide range of velocities and SNR.

1 System Model

A cyclic prefix single carrier block transmission (CP-SCBT) system is considered here and the slot structure is as follows:



where D represents the data symbol, and P represents a uniformly inserted pilot symbol with a guard interval to eliminate the ISI of channel estimation.

In Fig. 1, based on the pilots and the received signal, the channel coefficients are estimated and sent to the strongest path searcher. The searcher selects the strongest path and sends it to the Doppler shift estimator. The Doppler shift estimator computes the

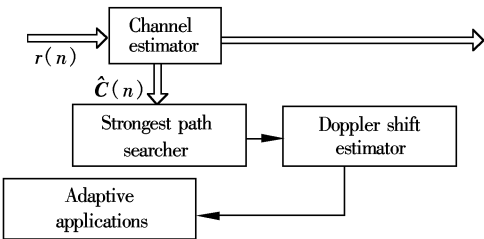


Fig.1 Doppler shift estimating part of receiver

Received 2003-10-08.
Foundation item: The National High Technology Research and Development Program of China (863 Program) (No. 2001AA123015).
Biographies: Hua Jingyu (1978—), male, graduate; You Xiaohu (corresponding author), male, doctor, professor, xhyu@seu.edu.cn.

Doppler shift for adaptive applications.

In the following it is assumed that the multi-path fading channels are wide-sense stationary and mutually uncorrelated scattering (WSSUS) processes so that each path can be estimated separately. After synchronously matching the pilot signal, the received fading signals of the l -th path can be written as

$$r_l(n) = c_l(n)d_p(n) + v(n) \quad (1)$$

where $c_l(n)$, $d_p(n)$ and $v(n)$ are channel parameters, pilot symbol and noise, respectively; and n is a discrete time index. Here $c_l(n)$ is modeled as a wide-sense stationary discrete-time complex Gaussian random process, and $v(n)$ is the zero-mean additive complex white Gaussian noise. An estimation of $c_l(n)$ based on (1) can be written as

$$\hat{c}_l(n) = \frac{r_l(n)d_p^*(n)}{|d_p(n)|^2} \triangleq c_l(n) + z(n) \quad (2)$$

where $z(n)$ is obtained after manipulating the white Gaussian noise $v(n)$ by the estimation process with variance σ_z^2 .

2 Doppler Shift Estimation

In this paper, five estimators of three types will be analyzed: ① Methods based on covariance characteristics including mean logarithm envelope difference (MLED)^[2] and autocorrelation function (ACF)^[5]; ② Methods based on envelope zero crossing rate (ZCR) of all orders including LCR^[6] and rate of minimum (ROM); ③ Methods based on channel phase characteristics including mean square phase difference (MSPD)^[8].

2.1 Estimator based on covariance

Since the original estimator of Ref. [2] is not suitable for wide bandwidth mobile communication systems, a new estimator based on MLED can be derived as follows:

$$\hat{f}_d = \begin{cases} \frac{-0.12 + 0.22\sqrt{0.46 + 0.45V}}{2\pi\tau} & 0 \leq V \leq 6.965 \\ \frac{V + 4.71}{38.5 \times 2\pi\tau} & V > 6.965 \end{cases} \quad (3)$$

where $V \triangleq \frac{1}{N} \sum_{i=0}^{N-1} (y_{i+1} - y_i)^2$, $y_i = 20\log_{10} |\hat{c}_l(i)|$, τ denotes the symbol duration, N represents the sample number and \hat{f}_d is the Doppler shift estimation.

We extend the estimator in Ref. [5] to a more general form as follows:

$$\hat{f}_d = \frac{1}{2M\pi\tau} J_0^{-1} \left(\frac{R(M)}{R(0)} \right) \quad (4)$$

where $R(k) = \sigma^2 J_0(2\pi f_d k\tau)$, $J_0(\cdot)$ denotes order 0 Bessel function of the first kind and $R(\cdot)$ denotes the ACF; k is the discrete time index; σ^2 is the channel mean power; M is a determinate positive integer. The inverse of $J_0(\cdot)$ is difficult in practice, but it can be realized approximately through a look-up-table or series extension. If a series extension is adopted, formula (4) can be rewritten as

$$\hat{f}_d \triangleq \hat{f}_{d,M} = \frac{1}{M\pi\tau} \sqrt{1 - \frac{R(M)}{R(0)}} \quad (5)$$

where $R(k) \approx \sigma^2 [1 - (\pi f_d k\tau)^2]$.

The approximation in formula (5) is accurate enough when $f_d k\tau < 0.15$. We choose $M=1$ to increase the estimation range.

2.2 Estimator based on ZCR of all orders

According to Ref. [6], LCR is approximately equal to the Doppler shift. Thus we can store K channel estimations of the l -th path, where K should be large enough to ensure that the time length T between the first and the K -th channel estimation is much larger than the fading periods. The Doppler shift can be estimated as^[6]

$$\hat{f}_d(n) \approx \frac{N_l(n)}{T} \quad (6)$$

where $N_l(n)$ is LCR.

ROM is analyzed in Ref. [9], and the Doppler shift can be estimated as

$$N_{\text{aprx}} = \frac{1}{2\pi} \sqrt{\frac{b_4}{b_2} + \frac{3b_2}{b_0}} = \frac{1}{2\pi} \sqrt{\frac{6\pi^4 \sigma^2 f_d^4}{2\pi^2 \sigma^2 f_d^2} + 3 \times \frac{2\pi^2 \sigma^2 f_d^2}{\sigma^2}} = 1.5f_d \quad (7)$$

$$\hat{f}_d = \frac{N_{\text{aprx}}}{1.5}$$

where $b_i (i=0, 2, 4)$ are the moments of channel power spectrum.

2.3 Estimator based on receiving signal phase characteristics

Assume $\varphi_n = \varphi(n\tau)$, where $\varphi(t)$ is the phase of the receiving signal. If a variable is defined as

$$\beta = \frac{1}{N} \sum_{n=1}^N (\varphi_n - \varphi_{n-1})^2 \quad (8)$$

then the Doppler shift can be estimated as follows^[8]:

$$\hat{f}_d = \begin{cases} \frac{0.012 + 0.21\beta}{\tau} & 0 \leq \beta \leq 0.619 \\ \frac{0.066 + 0.097\beta}{\tau} & 0.619 \leq \beta \leq 3.28 \end{cases} \quad (9)$$

For the sake of simplicity of notation, we call the MLED method estimator A, the ACF method estimator B, the LCR method estimator C, the ROM method estimator D, and the MSPD method estimator E. It must be noted that estimator A/C/D is robust enough to carrier frequency offset, and estimator B/E is robust enough to control power. Practically, we must choose estimators **according to our needs**.

3 Influence of Noise

The above estimators are obtained for a noiseless assumption, thus the estimation bias in noise case needs to be analyzed. The bias of estimator A is analyzed in Ref. [10]; here we will analyze other estimators.

We define the ratio factor of the Doppler shift estimation as

$$\eta_x = \frac{\hat{f}_{dN}}{f_{dI}} \quad x \in \{A, B, C, D, E\} \quad (10)$$

where f_{dI} denotes the estimate for a noiseless case, and f_{dN} denotes the estimate for noise case.

The ACF of noise case can be shown as

$$\left. \begin{aligned} R(1) &= \sigma^2 J_0(2\pi f_d \tau) + \sigma_z^2 \delta(\tau) = \sigma^2 J_0(2\pi f_d \tau) \\ R(0) &= \sigma^2 + \sigma_z^2 \end{aligned} \right\} \quad (11)$$

where $\delta(\cdot)$ is Dirac function. Thus ratio factor of estimator B can be simplified to

$$\begin{aligned} \eta_B &= \sqrt{\frac{1 - \frac{\sigma^2}{\sigma^2 + \sigma_z^2} J_0(2\pi f_d \tau)}{1 - J_0(2\pi f_d \tau)}} = \\ &= \sqrt{1 + \frac{1}{\gamma_s + 1} \frac{J_0(2\pi f_d \tau)}{1 - J_0(2\pi f_d \tau)}} \approx \\ &= \sqrt{1 + \frac{1}{\gamma_s + 1} \frac{1 - (\pi f_d \tau)^2}{1 - [1 - (\pi f_d \tau)^2]}} = \\ &= \sqrt{\frac{\gamma_s}{\gamma_s + 1} + \frac{1}{\gamma_s + 1} \frac{1}{(\pi f_d \tau)^2}} \end{aligned} \quad (12)$$

where symbol SNR is defined as $\gamma_s = \sigma^2/\sigma_z^2$. In appendix A, the ratio factor of estimator C/D is derived as

$$\left. \begin{aligned} \eta_C &= \sqrt{\frac{\gamma_s}{\gamma_s + 1} + \frac{1}{6(\gamma_s + 1)} \left(\frac{1}{f_d \tau}\right)^2} \\ \eta_D &= \sqrt{\frac{3\gamma_s + (1/(f_d \tau))^4/10}{9(\gamma_s + (1/(f_d \tau))^2/6)} + \frac{6\gamma_s + (1/(f_d \tau))^2}{9(\gamma_s + 1)}} \end{aligned} \right\} \quad (13)$$

Because the close-form expression of the ratio factor of estimator E is difficult to derive, the numerical results are used to show the influence of noise. Without loss of generality, the normalized

Doppler shift is defined as $f_m = f_d \tau$.

Fig.2 shows the Doppler shift estimation bias in noise case. It is obvious that higher SNR or more suitable bandwidth ratio $1/(f_d \tau)$ leads to a smaller bias. As Fig.2(d) shows, the MSPD of noise case is much larger than that of the noiseless case. In addition, we find that estimator D is more robust for SNR than other estimators although its bias is the largest.

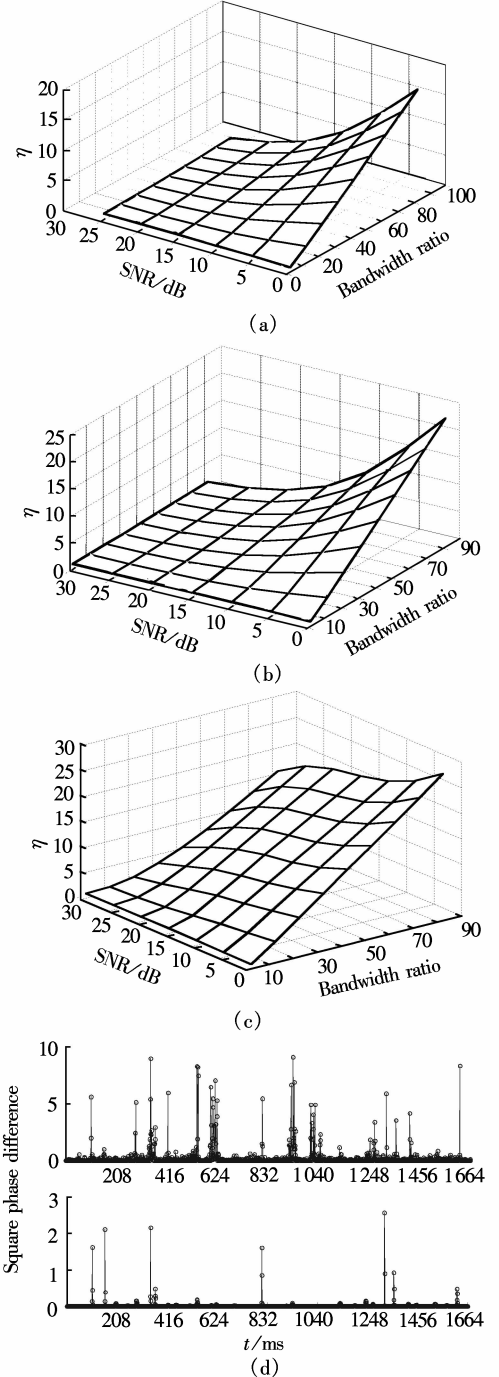


Fig.2 Ratio factors of the estimators. (a) Estimator B; (b) Estimator C; (c) Estimator D; (d) Estimator E

4 CRB for Doppler Shift Estimation

Generally, the objective is to find the minimum variance unbiased estimator (MVUE). As in Ref. [11], variance of MVUE must approach CRB if MVUE exists. Practically, MVUE is difficult to find and generic estimators are the approximation of MVUE in some special cases. Hence, comparing CRB with the variance of estimators is an important artifact to evaluate the estimator performance.

If the observed sequence satisfies the existing condition of CRB(see appendix B), CRB can be shown as^[11]

$$I(f_m) = 2\text{Re}\left\{\left[\frac{\partial \boldsymbol{\mu}(f_m)}{\partial f_m}\right]^T \boldsymbol{\Gamma}^{-1}(f_m) \left[\frac{\partial \boldsymbol{\mu}(f_m)}{\partial f_m}\right]\right\} + \text{tr}\left[\left(\boldsymbol{\Gamma}^{-1}(f_m) \frac{\partial \boldsymbol{\Gamma}(f_m)}{\partial f_m}\right)^2\right]$$

$$V_{\text{CRB}} = \frac{1}{I(f_m)} \quad (14)$$

where $\text{Re}\{x\}$ denotes the real part of x , V_{CRB} denotes CRB, $I(f_m)$ is the Fisher information, $\boldsymbol{\mu}(f_m)$ is the expectation vector of the observed sequence, and $\boldsymbol{\Gamma}(f_m)$ is the covariance matrix of the observed sequence. Considering Rayleigh channel, $\boldsymbol{\mu}(f_m)$ is zero and the following is derived:

$$[\boldsymbol{\Gamma}(f_m)]_{k,i} = R(k-i) = \sigma^2 J_0(2\pi f_m(k-i)) \quad (15)$$

5 Results and Analysis

The simulation parameters are shown in Tab.1.

Tab.1 Simulation parameters

Slot length/bit	1 056
Chip rate/(Mbit · s ⁻¹)	1.228 8
Pilot length/bit	32
Carrier/GHz	2.11
Coding	None
Channel model	M. 1225 model
Simulation time	1 000 slot
Path number	6
Pilot interval/ms	0.208
Modulation	QPSK

Fig.3 shows the accuracy of five estimators. It is obvious that the results will become more accurate if SNR or velocity increases, but the bias is large when speed is low, which is consistent with the analysis in section 3. When SNR is in the range of 5 to 10 dB, which is the effective SNR range for most mobile communication systems, the bias is tolerable. In addition, estimator A/E is more accurate than estimator

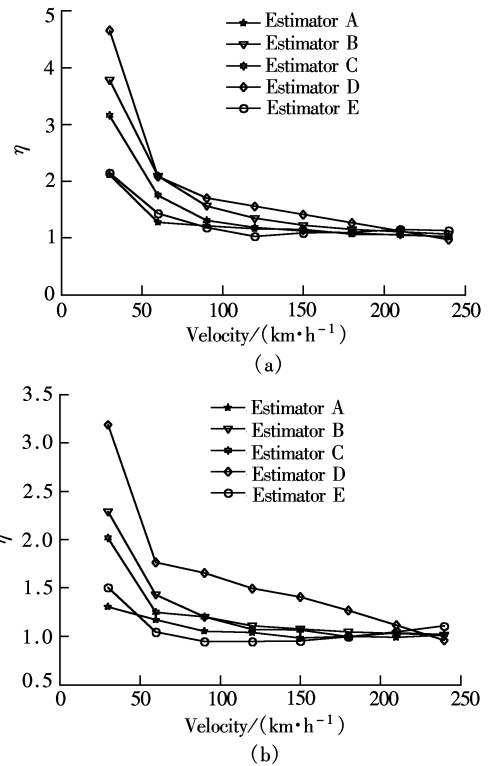


Fig.3 Doppler shift estimation accuracy. (a) SNR is 5 dB; (b) SNR is 10 dB

B/C/D.

Fig.4 illustrates the variance performance of the estimators, here variance is for the normalized Doppler shift. It is obvious that CRB for noise case is larger than that for the noiseless case. It can be easily found that estimator D has the largest variance, and variance of estimator A/B/C/E will be closer to CRB with increasing SNR. Moreover, the variance curves of estimator A/B/C/E are close to each other in high SNR (> 10 dB) and high speed (> 150 km/h), but the variance curves are remarkably distinguished from each other in other cases. To sum up, estimator A/E is better than estimator B/C/D. It must be noted that all five estimators are nonlinear estimators, thus un-bias is appropriate only for some specified speed ranges and SNR ranges, which cause some turns in Fig.4.

In Ref. [8], the authors propose a modification based on decimator, which increases the hardware complexity in a way. A simpler scheme is error prediction using polynomial fit; here we will take estimator C for example, and other estimators can be done analogously. Errors result from the SNR and from the relative error of low speed, which is higher than that of higher speed. Thus the revision will be based on these two aspects. Generally, communication systems work when SNR is larger than 5dB, thus we think the Doppler shift estimator works in high SNR (> 5 dB). In order to accomplish the fit operation, a

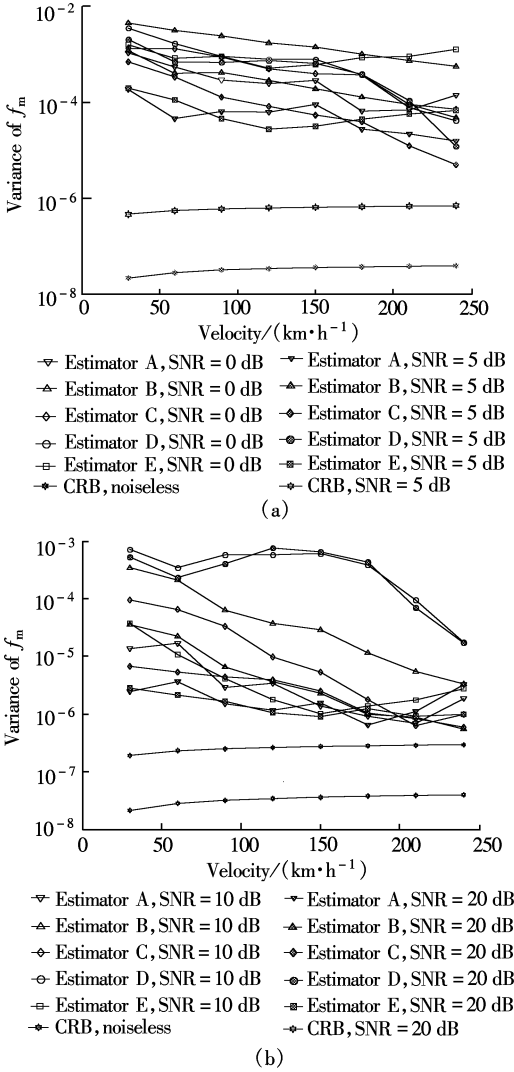


Fig.4 Variance performance of Doppler shift estimators.

(a) SNR is 0 dB or 5 dB; (b) SNR is 10 dB or 20 dB

table composed of the estimations for different SNR and velocity should be set up through simulation or on-line measurement, and then the relationship between the ratio factor and SNR or velocity can be found by numerical fit. After very cumbersome induction, the relative error prediction formula for speed can be summarized as

$$\hat{\sigma}_{f_d} = 3.54 \left(\frac{\hat{f}_d}{500} \right)^2 - 5.81 \left(\frac{\hat{f}_d}{500} \right) + 2.387 \quad (16)$$

where $\hat{\sigma}_{f_d}$ is the predicted relative error for speed. The relative error prediction formula for SNR can be computed as

$$\sigma_{f_d} = \frac{0.6619 \hat{\sigma}_{f_d}}{1.1604^{\text{SNR}-5}} \approx \frac{0.662 \hat{\sigma}_{f_d}}{1.16^{\text{SNR}-5}} \quad (17)$$

where σ_{f_d} is the final predicted relative error. Generally speaking, the Doppler shift estimation is larger than actual Doppler shift, thus the final modified Doppler shift estimation can be calculated as

$$\hat{f}_d = \hat{f}_d (1 - \sigma_{f_d}) \quad (18)$$

Fig.5 illustrates the performance of Eq.(18) and that of original estimator C. It is obvious that the estimation accuracy is improved greatly.

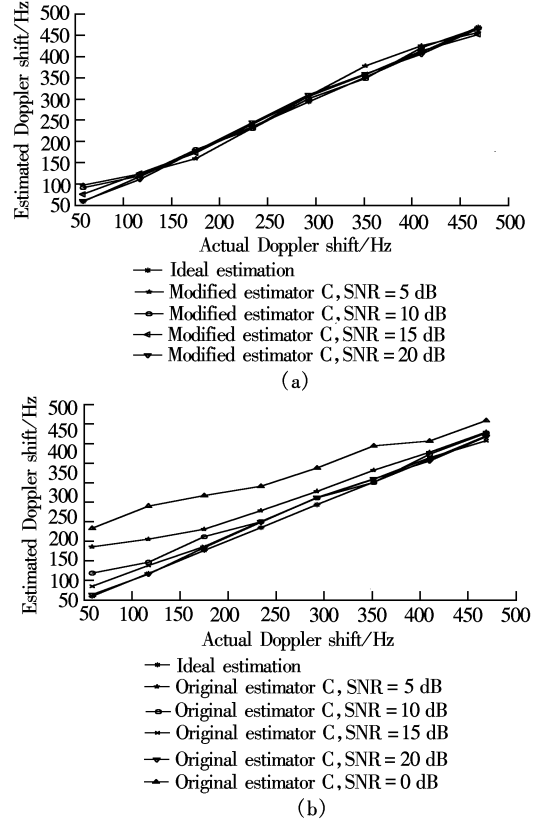


Fig.5 Doppler shift estimation with error prediction.

(a) Error predicted estimator C; (b) Original estimator C

Fig. 6 compares the original estimator C with error predicted estimator C. Large MSE gain can be found for error predicted estimator C, especially in low SNR, there is a gain of one order of amplitude when SNR is lower than 10 dB.

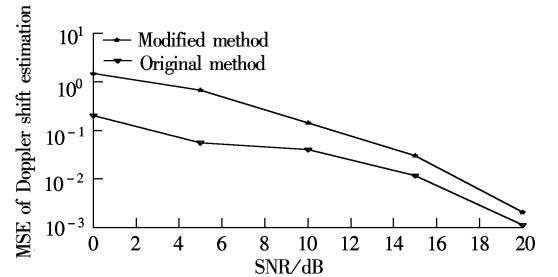


Fig.6 MSE performance for error prediction

6 Conclusion

The noise influence and applicable situations for some Doppler shift estimators in CP-SCBT system with time multiplexed pilot channel were discussed in this paper, and error prediction is proposed to degrade the

effects of noise. Simulation results show estimator A/E is the best and is robust with respect to carrier frequency offset and power control respectively. However, when we consider the complexity, estimator C is a good tradeoff between performance and **complexity, especially after modification.**

Appendix A

Here we will derive the ratio factor of estimator C/D. LCR can be shown as^[1]

$$N_{\text{LCR}} = \sqrt{\frac{b_2}{\pi b_0} - \frac{b_1^2}{\pi b_0^2}} \alpha e^{-\alpha^2}$$

$$b_n = (2\pi)^n \frac{\sigma^2}{\pi} \int_{-f_d}^{f_d} \frac{f^n}{\sqrt{f_d^2 - f^n}} df + (2\pi)^n \int_{-B/2}^{B/2} \frac{N_0}{2} f^n df$$
(A1)

where α denotes the ratio of threshold level and envelope root mean square (RMS) level. The classical U type channel power spectrum density (PSD) and AWGN with double PSD $N_0/2$ are assumed in formula (A1). Practically, noise bandwidth B is limited to $B = 1/\tau$.

b_2, b_1, b_0 for the noiseless case and noise case are calculated by choosing different values of N_0 . After substituting them into formula (A1) and (11), the ratio factor of estimator C can be rewritten as

$$\eta_c = \sqrt{\frac{\gamma_s}{\gamma_s + 1} + \frac{1}{6(\gamma_s + 1)} \left(\frac{1}{f_d \tau} \right)^2} = \sqrt{1 + \frac{(1/(f_d \tau))^2 - 6}{6(\gamma_s + 1)}}$$
(A2)

Analogous to estimator C, the ratio factor of estimator D can be written as

$$\eta_D = \sqrt{\frac{3\gamma + (1/(f_d \tau))^4/10}{9(\gamma + (1/(f_d \tau))^2/6)} + \frac{6\gamma + (1/(f_d \tau))^2}{9(\gamma + 1)}}$$
(A3)

Appendix B

Here we will prove that CRB of the Doppler shift estimator exists. Assume the conditioned probability density of observing vector \mathbf{x} is $p(\mathbf{x}, \theta)$, so regulation condition is^[11]

$$E\left[\frac{\partial \ln p(\mathbf{x}, \theta)}{\partial \theta}\right] = 0 \quad \text{for all } \theta$$
(B1)

Using the model of formula (2):

$$p(\hat{\mathbf{C}}_l, f_m) = \frac{1}{(2\pi\sigma_z^2)^{N/2}} \cdot \exp\left[-\frac{1}{2\sigma_z^2} \sum_{n=0}^{N-1} (\hat{c}_l(n) - c_l(n, f_m))^2\right]$$
(B2)

$$\frac{\partial \ln p(\hat{\mathbf{C}}_l, f_m)}{\partial f_m} = \frac{1}{\sigma_z^2} \sum_{n=0}^{N-1} (\hat{c}_l(n) - c_l(n, f_m)) \cdot \frac{\partial c_l(n, f_m)}{\partial f_m}$$
(B3)

Then we can conclude

$$E\left[\frac{\partial \ln p(\hat{\mathbf{C}}_l, f_m)}{\partial f_m}\right] = E\left[\frac{1}{\sigma_z^2} \sum_{n=0}^{N-1} z(n) \frac{\partial c_l(n, f_m)}{\partial f_m}\right] = \frac{1}{\sigma_z^2} \sum_{n=0}^{N-1} E\left[z(n) \frac{\partial c_l(n, f_m)}{\partial f_m}\right]$$
(B4)

Because $z(n)$ is independent of $c_l(n, f_m)$, thus $z(n)$ is independent of $\frac{\partial c_l(n, f_m)}{\partial f_m}$, then the right side of formula (B4) is 0; thereby CRB exists.

References

- [1] Jakes W C. *Microwave mobile communications* [M]. New York: IEEE Press, 1994.11 – 45.
- [2] Sampath A, Holtzman J. Estimation of maximum Doppler frequency for handoff decisions [A]. In: *Proc IEEE VTC* 1993 [C]. New York: IEEE Press, 1993.859 – 862.
- [3] Monk A M, Miltein L B. Open-loop power control error in a land mobile satellite system [J]. *IEEE JSAC*, **1995**, **13** (2): 205 – 212.
- [4] Cavers J K. An analysis of pilot symbol assisted modulation for Rayleigh fading channel [J]. *IEEE Transaction on VT*, **1991**, **40**(4): 683 – 693.
- [5] Xiao C, Mann K, Livier J. Mobile speed estimation for TDMA based hierarchical cellular systems [A]. In: *Proc IEEE VTC* 1999 [C]. New York: IEEE Press, 1999. 2456 – 2460.
- [6] Ma Zhangyong, Yan Yongqing, Zhao Chunming, et al. An improved channel estimation algorithm based on estimation level crossing rate for CDMA receiver [J]. *Chinese Journal of Electronics*, **2003**, **12** (2): 235 – 238. (in Chinese)
- [7] Kawabata K, Nakamura T, Fukuda E. Estimating velocity using diversity reception [A]. In: *Proc IEEE VTC* 1994 [C]. New York: IEEE Press, 1994. 371 – 374.
- [8] Hua Jingyu, You Xiaohu. A scheme for the Doppler shift estimation despite the power control in mobile communication systems [J]. *Chinese Journal of Communication*, **2004**, **25**(5): 1 – 6. (in Chinese)
- [9] Rice S O. Mathematical analysis of random noise [J]. *Bell Syst Tech J*, **1945**, **24**(1): 46 – 156.
- [10] Tepedelenioglu C, Giannakis G B. Estimation of Doppler spread and signal strength in mobile communications with application to handoff and adaptive transmission [J]. *Wirel Commun Mob Comput of Wiley*, **2001**, **1**(2): 221 – 242.
- [11] Kay S M. *Fundamentals of statistical signal processing: estimation theory* [M]. New York: Prentice Hall, 1993.27 – 45.

移动通信中的多普勒频偏估计方法

华惊宇 尤肖虎

(东南大学移动通信国家重点实验室, 南京 210096)

摘要: 针对几种多普勒频偏估计方法,分别为对数包络法、自相关函数法、各阶电平通过率法和均方相位差分法,在理论上分析了瑞利信道中它们的估计原理和估计偏差,说明了这些估计方法各自的适用场合. 同时推导了多普勒频偏估计器的 CRB (Cramer Rao bound),并且提出了一种新的利用二阶多项式拟合的修正方法以提高多普勒频偏估计精度. 算法验证采用蒙特卡罗计算机仿真,结果表明,相对于原始估计方法,拟合修正后的方法估计性能得到了较大的提高.

关键词: 多普勒频偏; 后三代 (B3G); CRB

中图分类号: TN929.533